

Full Length Article

Diamane quasicrystals

Leonid A. Chernozatonskii ^{a,*}, Victor A. Demin ^a, Alexander G. Kvashnin ^b, Dmitry G. Kvashnin ^a^a Emanuel Institute of Biochemical Physics, Russian Academy of Sciences, 4 Kosigin St, Moscow 119334, Russian Federation^b Skolkovo Institute of Science and Technology, Skolkovo Innovation Center, 30 Bolshoy Boulevard, bld. 1, 121025, Moscow, Russian Federation

ARTICLE INFO

Keywords:

Quasicrystal
Diamane
Twisted bigraphene
Density functional theory
Electronic structure
Mechanical properties

ABSTRACT

Here we propose the first two-dimensional carbon quasicrystal made entirely of sp^3 -hybridized atoms, namely diamane quasicrystal. This nanostructure is based on incommensurate lattice of two graphene layers twisted by 30° with respect to each other (well-known graphene quasicrystal) with totally hydrogenated or fluorinated surfaces of bilayer graphene (similar to formation of AB-stacked diamane by means of applying high pressure treatment). We describe in detail the features of atomic structure appearing during the formation of quasicrystal. Thermodynamic stability, electronic and mechanical characteristics in comparison with both periodic approximants and AB-stacked diamanes via DFT and MD methods are studied and discussed. Proposed diamane quasicrystals exhibit unique mechanical properties: they are stiffer and more brittle than AB-stacked diamane. Our study shows that quasicrystalline diamane is a prospective material that opens a new way towards the synthesis of inorganic quasicrystals of various compositions with unique set of physical and chemical properties.

1. Introduction

Quasicrystals (QCs) are of great interest to researchers since their discovery by Dan Shechtman in 1984 [1], which opened a new field of materials science owing to unique 3D structures and their properties [2]. QCs are structures with quasi-periodic orders without spatial periodicity. Since the discovery, the existence of hundreds of quasicrystals has been reported and confirmed [2]. In 2018 the first two-dimensional (2D) quasicrystals, graphene quasicrystals (GQC), based on two twisted molecularly bonded graphene layers with a twist angle of exactly 30° [3–6] were prepared by micromechanical exfoliation [7]. This method was used for the synthesis of metallic 2D quasicrystalline layers of Ta_{1.6}Te and Al₆₆Co₁₇Cu₁₇ performed by Zettl [8] and Ajayan [9] groups. The structure of GQC can be described as a Stampfli tile map [10]. New effects related to the formation of quasi-2D structure and its advantages and properties are still in the intensive theoretical study stage [3,5,11–13].

However, graphene quasicrystal is described as an extrinsic quasicrystal, which is based on a pair of perfect 2D crystals with independent periodicities. Graphene quasicrystal has no chemical bonding between the layers in contrast to known intrinsic 3D QCs [2] and its 2D counterparts [8,9], where atomic sites are intrinsically arranged in the quasiperiodic order. The top projection of the atomic structure of GQC on a plane is described by QC lattice with 12-fold symmetry which was

firstly considered by Stampfli [10]. Mentioned above features of the atomic structure of GQC lead to the appearance of a number of Dirac cones in the band structure [3–6,8,9,11–13], which make GQC promising material for tunable electronics.

Ultrathin diamond films based on AA- or AB-stacked graphene layers [14–18] named diamanes are wide gap semiconducting quasi-2D materials with high stiffness and hardness comparable to diamond [17–21]. Moreover, the twist of graphene layers with respect to each other with the following formation of Moiré diamanes through the hydrogen or fluorine passivation of outer surfaces leads to the remaining of its insulating properties with the band gap wider than that of AB-stacked diamanes [22]. Partial functionalization of Moiré bilayers of graphene with the band gap of 1.21 eV was considered theoretically starting from 2012 by Muniz and Maroudas group [23,24].

The formation of covalent interlayer bonds was experimentally observed in cold-compressed graphite at the pressure of ~17 GPa and room temperature [25]. Pressure initiates the transformation of half of the sp^2 -hybridized carbon atoms (π -bonds) to sp^3 (σ -bonds). Rajasekaran et al. [26] confirmed by X-ray absorption spectra that hydrogenation of the top graphene layer deposited on the substrate leads to structural changes indicating the formation of covalent bonds between the layers. This experiment totally confirmed previous theoretical studies [17] that suggested the key role of chemical functionalization in the formation of covalent bonding between graphene layers. Mentioned above facts state

* Corresponding author.

E-mail address: chernol-43@mail.ru (L.A. Chernozatonskii).

the possibility of chemical conversion of multilayered van der Waals structure into a quasi-2D covalently bounded film with controlled thickness depending on an initial number of graphene layers. Similar effects confirmed by Raman spectroscopy were already observed during one-side hydrogenation of multilayered graphene [26–29]. Moreover, it was reported about a number of theoretical and experimental studies of fully fluorinated multilayered graphene [15,30–32]. Recent studies [21,33,34] have reported on the observation and possibility to synthesize the thinnest possible films with diamond structure using high-pressure-high-temperature treatment of bilayered or multilayered graphene.

During the last decade, quasi-2D diamond films were confirmed by a set of experimental techniques [35], including transmission electron microscopy, Raman spectroscopy, and X-ray diffraction. The development of pressure-free methods for the formation of diamanes initiates a drastic increase of interest in their properties and possible applications.

Here we propose a novel intrinsic 2D quasicrystal based on fully hydrogenated or fluorinated bilayer graphene with a twist angle of 30° and interlayer covalent bonding. This nanostructure is a diamane quasicrystal, which completely consists of sp^3 -hybridized carbon atoms. Unique atomic geometry was carefully analyzed and described. The stability of the atomic structure, as well as acquired electronic and mechanical properties, were studied using computational techniques based on DFT and MD approaches.

2. Computational details

Geometry relaxation of considered quasicrystalline diamanes and calculations of electronic properties were performed using the VASP [36–38] package. The generalized gradient approximation with the Perdew-Burke-Ernzerhof parametrization [39] of exchange–correlation functional within the projector-augmented wave method [40,41] was used. The plane-wave energy cutoff was set to 500 eV. The smallest allowed spacing between k-points is 0.25 Å⁻¹. 1D and 2D systems were separated from their periodic images by a vacuum region of more than 10 Å to avoid the artificial interaction between them. Atomic structure minimization was carried out until the change in total energy was less than 10⁻⁴ eV. It should be taken into account that the generalized gradient approximation used in our work leads to systematic underestimation of the band gap, for example, for pure diamond the experimental value is 5.47 eV [42] and the calculated one is 4.2 eV.

A well-developed theoretical approach of Brenner bond-order potential [43] was used to study mechanical properties of considered 2D QC through the simulation of the indentation process. These simulations were performed using a LAMMPS package [44]. Considered QC and diamane clusters had a circular shape with a diameter of ~3 nm and fixed boundaries, and were deflected by an indenter of fixed atoms with conical shape and the mean diameter of 1/5 of the film diameter. Interaction between structure and the tip has pure repulsive nature. The deflection was carried out with at 0.1 Å intervals. Before and during each step of the mechanical test the atomic structure was relaxed by conjugated gradient minimization while the maximum interatomic forces became less or equal to 0.05 eV/Å. We successfully used this approach in our previous works [17,18,45].

3. Results and discussions

3.1. Features of fully passivated graphene layers with the twisted angle of 30° – Quasicrystal diamane

Here we propose and study the structure of fully hydrogenated or fluorinated covalently bonded bilayer graphene with a relative interlayer twist angle of 30° – DnQC (Diamane QuasiCrystal). The incommensurate atomic structure of GQC with Stampfli tiling is presented in Fig. 1a. A unique feature of proposed structure is the presence of only in-plane carbon bonds in each graphene layer, which are rotated with respect to each other by 90°. In DnQC the adsorption of hydrogen or fluorine atoms to the carbon atoms leads to the formation of crossed interlayer bonds, which form the X-C-C-X (X = H/F) “boat” complexes. On the other hand, neighboring to the “crosses” carbon atoms could create covalent bonds with carbon atoms of another layer like in ordinary AB-stacked diamane (see bottom panel of Fig. 1b). Experimental pieces of evidence and theoretical calculations of possibility of hydrogen or fluorine adsorption on graphene [46,47] and Moiré bilayer graphene [22,48] confirm the possibility of formation of X-C-C-X “boat” complexes. The formation of X-C-C-X “boat” complexes during the adsorption of hydrogen or fluorine atoms on the surface of AA'-stacked bilayered graphene was theoretically predicted [18,28] and experimentally proved in the case of multilayer graphene surfaces during hydrogenation [46] or fluorination [47]. Thus, the proposed DnQC structure is justified by the experimental and theoretical data mentioned above. In contrast to single crystal diamond and AB- or AA-stacked

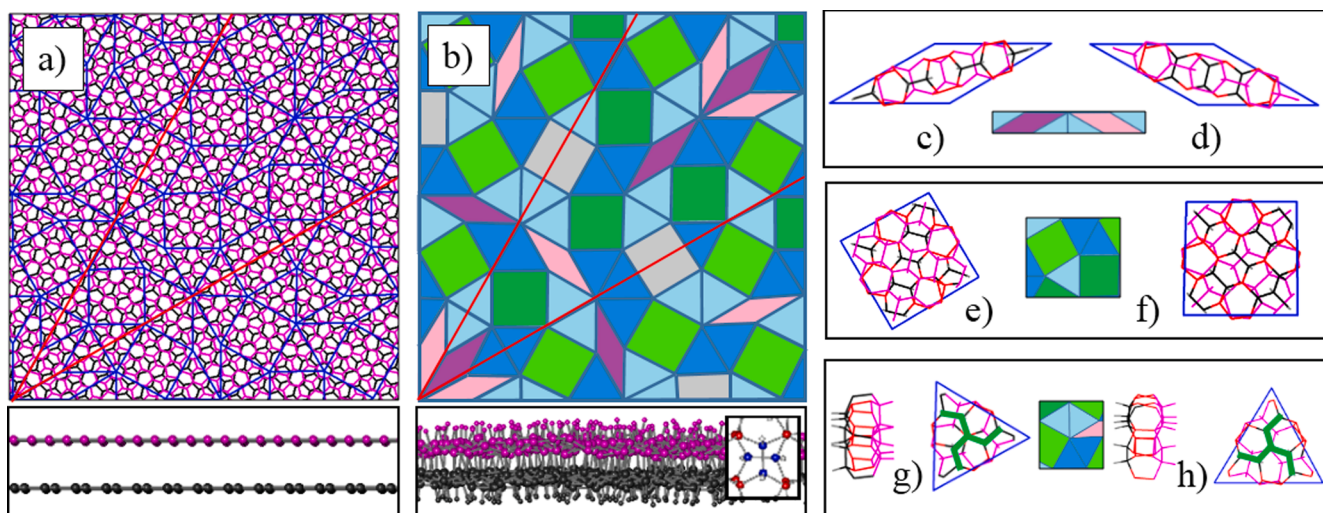


Fig. 1. Top and side views of (a) Stampfli tile of bilayer graphene and (b) reconstructed Stampfli tile of diamane quasicrystal structures (b – with a cross of two H-C-C-H complexes). Carbon and hydrogen atoms of the top and bottom layers are marked by violet and black colors, respectively. Stampfli tile lattice in (a) is marked by blue lines. The sector with 12-folded symmetry of the structure is marked by red lines in (a). Six-fold symmetry sectors in (b) are marked by red lines. Equilateral elements in (a) and (b) are highlighted by light and dark colors. Atomic structure of violet rhombuses (c,d), green squares (e,f) and blue triangles (g,h). Interlayer bonds are marked by red.

diamanes, all carbon bonds in DnQC have various spatial orientations and bond length distributions (see Fig. S1 in Supporting Information). This distribution is similar to the sp^3 -bonded tetrahedral carbon structure of amorphous diamond [49]. Thus, it is possible to state that the proposed DnQC could be considered as the thinnest 2D quasi-amorphous diamond film.

It should be noted that Stampfli described only pure 2D flat structure with 12-fold symmetry based on two mutually twisted hexagonal lattices [10] containing a set of identical elements: rhombuses, squares and triangles (Fig. 1a). The structure of GQC could be associated with Stampfli tile only in the case of plane projection (top view), while in fact GQC has a thickness and therefore 3D structure of GQC has lower rotational 6-fold symmetry. Symmetry decreasing leads to a reconstruction of Stampfli tiling (Fig. 1b, reconstructed Stampfli Tile, rST) and separation of the elements into several types. It should be noted that experimentally (e.g. Raman spectroscopy, low-energy electron microscopy/diffraction, transmission electron microscopy) the structure of GQC is usually interpreted as the same as Stampfli tile with 12-fold symmetry [3,4] due to the absence of possibility to distinguish elements of identical shape. Only rotation of rST with respect to the normal by 60° detects translational transition into itself. The view of this rST can return to the original ST view if the third dimension of this quasi-two-dimensional crystal will be withdrawn from consideration. Symmetry decreasing of bilayer graphene from 12- to 6-fold will be especially noticeable after the adsorption of atoms on its surface and subsequent connection of layers with the following formation of DnQC (Fig. 1b). Therefore, the DnQC structure has 6-fold symmetry according to the 3D nature of the tiles which have a different structure of X-C-C-X complexes on the surfaces (Fig. 1c-h). We highlighted by light and dark color two types of equilateral tiles in Fig. 1b. Considered rST map has inflation similar to the case [3,10] which presented in Fig. S2. So DnQC has rough surfaces unlike GQC and AB-diamane surfaces as well. In the case of DnQC, there is a non-periodic distribution of C-H bonds. Diamane structure can be imagined like a four-layer C-atom structure – outer layers that are hydrogenated or fluorinated and inner layers of atoms that are connected between each other by interlayer bonds. This fact is important for the identification of diamane structure by diffraction methods.

Let us consider the new elements of reconstructed Stampfli tiling in detail. There are two types of elements of Stampfli tiles: rhombuses, equilateral triangles, and squares in a sector that coincides with itself after the rotation by a specific angle corresponding to the 6-fold

symmetry of considered DnQC. Two rhombuses (Fig. 1c,d) are marked by dark and light violet colors in Fig. 1b composed of a chain of hexagons. The top and bottom layers of the dark-colored element consist of chains of three hexagons with zigzag and armchair edges, respectively. In such configurations, the X-C-C-X complexes are aligned along the main diagonal of the bottom layer and perpendicular in the top layer with connections of the layers via their edges (Fig. 1b). The same configuration was observed for the light violet elements with the only difference that the description of the top layer of the light violet element corresponds to the bottom layer of the dark element and vice versa. Square elements contain crosses of the bonds from the top and bottom layers in the center of the element (green and gray colors, see Fig. 1e,f for details and Fig. 1b for their distribution). All squares have the same structure but have different mutual orientations. Each triangle element has an interlayer bond located in the center and three crossed bonds at the triangle corners (Fig. 1g,h). These elements have three X-C-C-X complexes which are arranged by clockwise rotation (marked by green lines in Fig. 1g,h) in the top and counterclockwise rotation in the bottom layers, respectively. Light elements have the same structure as dark ones, but the top and bottom layers are reversed.

For the complete description of DnQC, we defined seven joining points of the elements marked by squares in Fig. 2a. Each element is made of two hexagons at the center of the element located in both layers lying on top of each other. The first region (I in Fig. 2b) has only rhombuses which intersect in a single point locating at the center of the element. There are no interlayer covalent bonds (C-C', where prime denotes carbon atom from another layer) between hexagons at the center of the structure. All carbon atoms are functionalized as a fullerene-like C_{48} cluster. The second region (II in Fig. 2b) is represented as two rhombuses intersect with a triangle (five C-C' covalent bonds, red atoms in Fig. 2b); the third region (III in Fig. 2b) contains rhombus, four triangles and one square (four C-C' bonds in total). The fourth region (IV in Fig. 2b) has the joining point with three triangles and two squares (three C-C' bonds). The fifth region (V in Fig. 2b) is a connection between five triangles (blue) and two rhombuses (violet) and has five C-C' bonds. The sixth region (VI in Fig. 2b) is a joining point of two triangles, rhombus and square (four C-C' bonds); the seventh region (VII in Fig. 2b) has the same number of triangles (four) as in III and four rhombuses (four C-C' bonds in the central hexagon). Based on the above description it is possible to define four main C-C' configurations with different adsorbed atoms in central hexagon (Fig. 2). The II and V schemes have the same number of covalent bonds between the layers

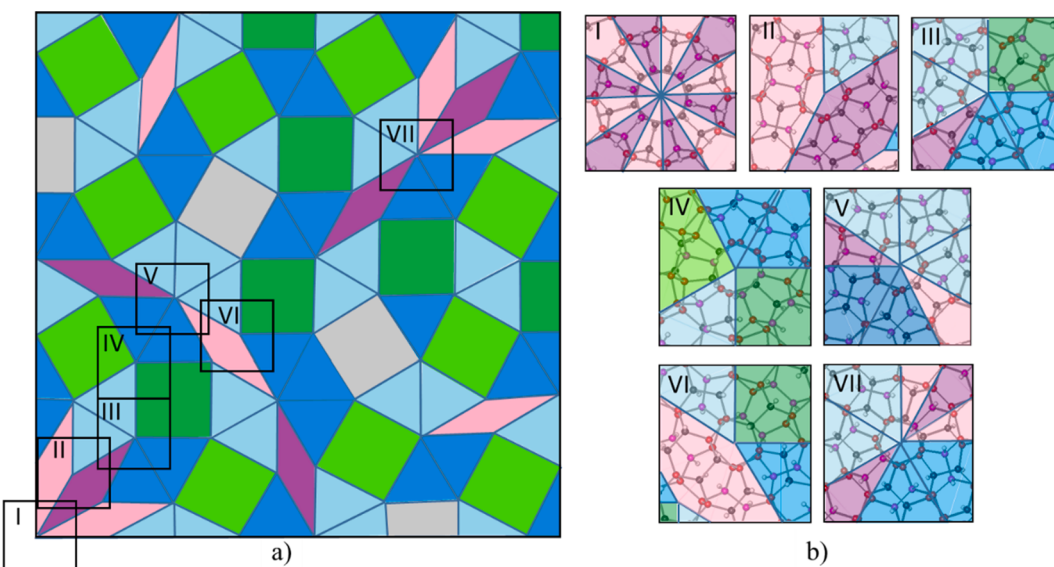


Fig. 2. (a) Reconstructed Stampfli tile of diamane quasicrystal and (b) schematic illustration of each element and their joining points.

(five C-C' bonds). The III, VI and VII schemes have four C-C' bonds. That is why all DnQC structures have four types of joining points only.

A detailed description of the atomic structure of DnQC and structural elements allow us to conclude about the wide variety of possible configurations depending on the number of joining points and structural features of reconstructed Stampfli tiling. Different local symmetry of joining points of structural elements leads to different electron distribution and appearance of energy levels in the electronic energy spectrum of DnQC clusters.

3.2. DnQC and its approximant models

It is important that DnQC has only rotational symmetry and no translational ones. To study the atomic structure and electronic properties of DnQC, as in the case of GQC [8], it is necessary to choose finite models and possible commensurate approximant. Therefore, we considered finite-size nanoclusters which were selected from different parts of the DnQC (see Fig. 3). All considered clusters have a circular shape with a diameter of 1.6 nm. The first cluster $C_{516}H_{312}$ was selected from the DnQC center (Fig. 3a). The second one ($C_{516}H_{328}$) was selected from the point located in the joining point with four triangles and four rhombuses (VII in Fig. 2b). Atomic structures of considered clusters are presented in Fig. 3a,c. All dangling bonds located at the edges of a cluster were passivated by hydrogen. Results of DFT calculations of their electronic densities of states (DOS) are shown in Fig. 3b,d. It was found that DnQC clusters display insulating properties with HOMO - LUMO energy difference (analogue of band gap in crystal) $E_{\text{HOMO}} - E_{\text{LUMO}} \sim 3.2$ eV. For comparison, we calculated the electronic properties of a smaller cluster ($C_{168}H_{120}$) selected from the center of the DnQC as well. Cluster $C_{168}H_{120}$ has larger $E_{\text{HOMO}} - E_{\text{LUMO}} \sim 3.4$ eV (see Fig. S3b in Supporting Information) due to more strained bonds between atoms (see bond length distribution in Fig. S1c in Supporting Information).

To make a comparison with electronic properties of various diamanes the only way is to choose a periodic approximant structure. Here we choose Moiré diamane with a twist angle between the top and bottom layers of 29.4° (Dn29.4, Fig. 3e) due to relatively small unit cell ($C_{388}H_{174}$), which is reliable for DFT calculations. Approximant Dn29.4 is considered to extrapolate an incommensurate structure to an infinitely large cell, because, as it was shown earlier [11], the density of states of

bigraphene with twist angles of 29.01° - 29.98° matches the electronic DOS of GQC. The structure of the Dn29.4 is described in detail in Ref. [22]. Based on this we could state that Dn29.4 should give good a description of the main peculiarities of DnQC electronic properties. The band gap of the Dn29.4 approximant is 3.6 eV (see Fig. 3f). An increase of the band gap in comparison with AB-stacked diamane (3.1 eV) is associated with an increase of the number of strained C-C' bonds. All interlayer bonds in AB diamane are equivalent and oriented normally to the surface. Interlayer bond lengths of approximant Dn29.4 (Fig. S1b in Supporting Information) are distributed from 1.50 to 1.66 Å with various spatial orientations which differs from normal. Thus, we can conclude that the band gap of the DnQC should be larger than ~ 3.5 eV, which is smaller than the corresponding value for diamond (4.2 eV) and larger than that of AB diamane (3.1 eV) [22].

3.3. Diamane quasicrystal based on fluorinated GQC

Recently Li et al. [47] applied a nanosized electron-beam-induced deposition process to decompose XeF_2 precursor molecules with a subsequent synthesis of CF-film from free-standing graphene after a short time. We expect that a similar technique could be very efficient for the synthesis of F-DnQC. Since fluorine atoms bind stronger to carbon than hydrogen atoms, fluorinated structures (fluorinated graphene, fluorinated diamane, F-Dn) are usually more stable compared to hydrogenated ones. This indicates that fluorinated F-DnQC may be obtained easily than hydrogenated DnQC discussed above.

To estimate the band gap of fluorinated quasicrystal we considered the same Dn29.4 approximant structure with fluorinated surfaces and a finite-size cluster $C_{168}F_{120}$ which was selected from the center of F-DnQC. Comparison of bond lengths distribution of fluorinated and hydrogenated clusters (Fig. S1c,d) shows that fluorinated cluster has a greater diversity in bond lengths than hydrogenated one. This fact states about increasing of HOMO - LUMO energy difference to ~ 3.7 eV ($E_g = 3.2$ eV for $C_{168}H_{120}$ cluster), but with the localized energy level at 3 eV. The fluorinated periodic approximant also has a larger band gap of 4.1 eV than $E_g = 3.6$ eV for hydrogenated Dn29.4. Thus, F-DnQC should have a band gap over 4 eV, which is comparable to the value of diamond and significantly exceeds the values of hydrogenated diamane structures.

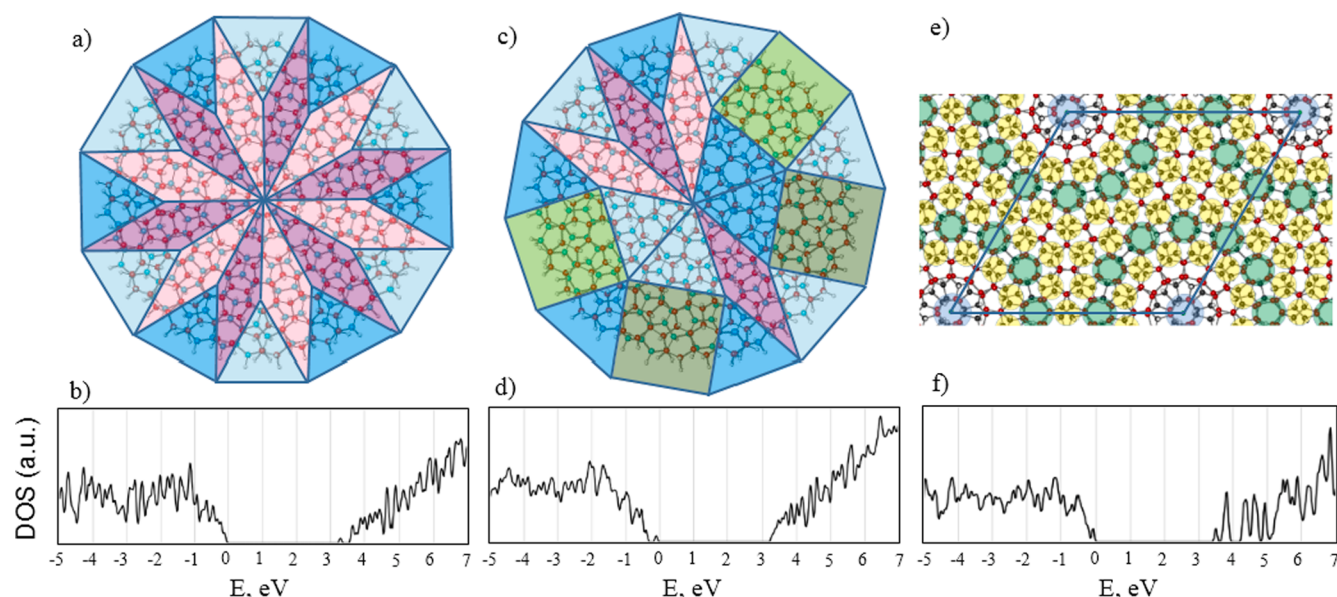


Fig. 3. Structure of the diamane quasicrystal clusters $C_{516}H_{312}$ and $C_{516}H_{328}$ with the center coinciding with (a) the center of DnQC and (c) joining point VII with four triangles and four rhombuses, and their corresponding electronic densities of states (b,d). Structure of the periodic approximant Dn29.4 (e) and its electronic density of states (f).

3.4. Energy stability of DnQC in comparison with other sp^3 carbon materials

To study thermodynamic stability of considered quasicrystalline diamane structures we calculated the energy of formation as follows:

$$E_f = \frac{E_{tot} - M \cdot E_G - \frac{N}{2} E_{X_2}}{M + N}$$

where E_{tot} , E_G , and E_{X_2} are the total energies of the considered Dn structure, carbon atom in graphene, and X_2 ($X = H, F$) molecule, respectively; M and N are the number of carbon and X atoms, respectively.

The results of calculations for the considered above systems and other known compounds are presented in Fig. 4. The presence of strained interlayer bonds leads to higher E_f for the twisted Dns and DnQC clusters in comparison with AB-stacked diamane. However, hydrogenated twisted Dn is approximately as stable as diamond. DnQC clusters are more stable than diamanes based on commensurate bigraphene layers with various twisted angles. Fluorinated diamanes have lower energy of formation than hydrogenated ones (red circles in Fig. 4). Stoichiometry, energies of formation and band gaps of all calculated structures are presented in Table S1 (see Supporting Information).

3.5. Mechanical properties of DnQC

Another important property of 2D diamane-like films is behavior under critical deformation [17,18]. To describe the behavior under critical deformations the nanoindentation process of DnQC was simulated, which repeats the experimental setup from Ref [50]. It was found that AB-stacked diamane appeared to be stronger than grapheme and graphane and has a much larger stiffness coefficient [17]. Therefore, the mechanical response of proposed DnQCs and diamane with AB stacking under indentation loading was studied.

The mechanical response of diamanes under indentation is represented by increasing indentation force with deflection of the film. The whole nonlinear force-deflection dependence can be used for the calculation of the stiffness coefficient E^{2D} using the following relation [45,50,51]:

$$F(\delta) = \sigma^{2D}(\pi a) \left(\frac{\delta}{a} \right) + E^{2D} \left(q^3 a \right) \left(\frac{\delta^3}{a^3} \right),$$

where δ is the depth of deflection of the atom in the center of the

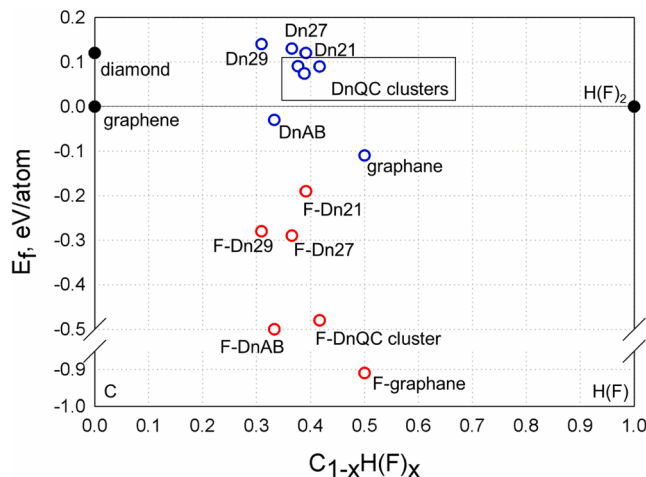


Fig. 4. Energy of formation as a function of a number of adsorbed atoms (hydrogen or fluorine) with respect to graphene. Energy of the formation of graphene is taken as zero. Data for graphene, diamond and X_2 molecules are shown by black circles, while hydrogenated and fluorinated structures are shown by blue and red circles, respectively.

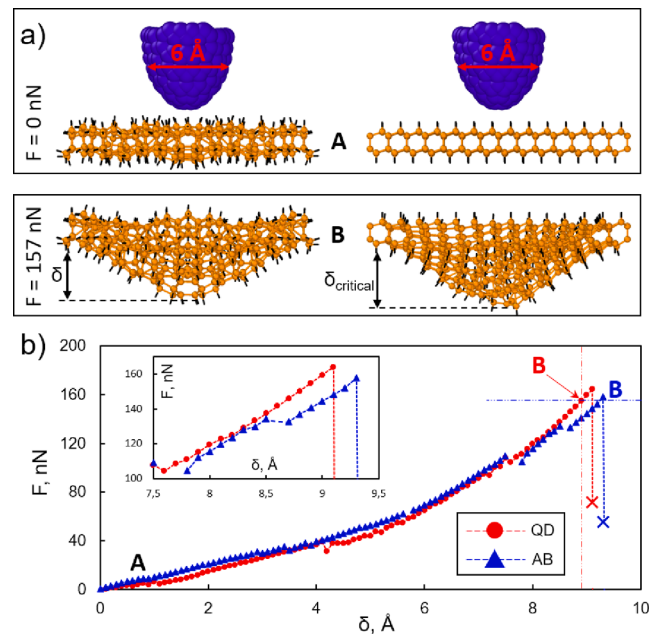


Fig. 5. (a) Main steps of indentation process of QD (cut from the rST center - left) and AB diamane (right) membranes with a diameter of 3.0 nm; (b) dependence of indentation force on the deflection depth. Dependences for QD and AB diamane are presented by red and blue curves. Initial and critical states are depicted by A and B letters.

diamane film, a is the diamane radius, $q = (1/(1.05 - 0.15\nu - 0.16\nu^2))$ is a dimensionless constant which depends on Poisson ratio. Here we used Poisson ratio of diamond equal to 0.2 [50], σ^{2D} is the pretension of the film.

In Fig. 5a, the result of nanoindentation for DnQC (left) and DnAB (right) is shown at different penetration ratios (δ). The force–deflection dependence was calculated from the indentation process. A short analysis of obtained curves shows linear behavior of F vs. δ in the region of penetration depth up to 5 Å, while further loading leads to a non-linear regime at large deflection. Analysis of bonds density shows that the C-C density in the DnQC structure is 19% higher than in DnAB (1.88 and 1.57 bonds per Å^2 for QD and AB, respectively). This fact and obtained data show that DnQC is stiffer than DnAB (it is required to apply greater force to indent DnQC film, Fig. 5b, red curve).

To study mechanical characteristics, we calculated 2D elastic constant E^{2D} by taken the derivative from the indentation force and express E^{2D} as:

$$E^{2D} = \frac{4ba^2}{q^3}$$

where b is the coefficient of the fourth-order term in polynomial dependence for the energy-deflection curve. Estimations show that the stiffness constant of the DnQC structure is higher than in AB diamane by 16%.

4. Conclusion

Here we proposed a new diamane quasicrystal obtained based on reconstructed Stampfli tile with 6-fold rotation symmetry caused by non-zero thickness. A detailed analysis of the atomic structure was carried out and the main structural elements were identified. We studied the electronic properties of considered DnQC and the approximant of Moiré diamane Dn29.4 by using DFT calculations. It was found that calculated band gap values were larger than for AB-stacked diamanes ($E_g = 3.1$ eV) and equal to 3.5 eV. The increasing band gap is associated with the presence of strained C-C interlayer covalent bonds which are

not purely sp^3 -hybridized as in the cases of diamond and AB diamane structures. The study of mechanical properties shows that DnQC is mechanically stronger than AB diamanes. Moreover, fluorinated diamane quasicrystals are energetically preferable to hydrogenated ones. We expect that the last experimental advances of synthesis of AB diamanes will be applied to synthesize different Moiré diamanes.

This research opens a new field of materials science related to investigations of two-dimensional quasicrystals of various compounds. Obtained results on the structure of diamane quasicrystals can be applied to study 2D covalent quasicrystals made of other bilayer materials with honeycomb lattice and a twist angle of 30° . For instance, it could be quasicrystal based on the bilayer of h-BN, silicene and other materials fabricated by functionalization by different adsorbents including chlorine, bromine [52], or already mentioned hydrogen or fluorine. It can be *diamanone* quasicrystal which is formed by adsorption of hydrogen or fluorine on the graphene quasicrystal only on one side, while the other side is connected to a flat substrate. We also hope that it is possible to synthesize *diamene* (diamane without any passivation) quasicrystal by applying external pressure to multilayer graphene similar to the formation of diamond-like films from ordinary AB-stacked bigraphene [21,34]. However, the presence of C-C sp^2 -hybridized pairs instead of X-C-C-X of complexes in such compressed 2D QC will lead to a narrowing of the band gap.

All these results provide potential resources for the construction of new 2D wide-gap dielectric materials and devices. Along with ultrawide-gap resonance optical properties of DnQC - devices on resonant absorption, due to the combination of the DOS spectrum by choosing high DOS peaks we can get strong absorption or nonlinear optical responses in the ultraviolet region. We can state that considered diamane quasicrystals can be applied for the fabrication of the new graphene-based optics and electronic nanoelements.

CRediT authorship contribution statement

Leonid A. Chernozatonskii: Conceptualization, Methodology, Supervision, Project administration, Funding acquisition, Writing – original draft. **Victor A. Demin:** Methodology, Software, Investigation, Writing – original draft. **Alexander G. Kvashnin:** Methodology, Software, Investigation, Writing – review & editing. **Dmitry G. Kvashnin:** Methodology, Software, Investigation, Writing – original draft.

Declaration of Competing Interest

The authors declare that they have no known competing financial interests or personal relationships that could have appeared to influence the work reported in this paper.

Acknowledgements

Authors are grateful to Prof. K.S. Novoselov for discussion and comments. This work is supported by the Russian Foundation of Basic Research (№20-02-00558). The calculations were performed using the resources provided by the Joint Supercomputer Center of the Russian Academy of Sciences.

Appendix A. Supplementary data

Supplementary data to this article can be found online at <https://doi.org/10.1016/j.apsusc.2021.151580>.

References

- [1] D. Shechtman, I. Blech, D. Gratias, J.W. Cahn, Metallic Phase with Long-Range Orientational Order and No Translational Symmetry, Phys. Rev. Lett. 53 (20) (1984) 1951–1953, <https://doi.org/10.1103/PhysRevLett.53.1951>.
- [2] W. Steurer, Quasicrystals: What do we know? What do we want to know? What can we know? Acta Crystallogr. A Found. Adv. 74 (2018) 1–11, <https://doi.org/10.1107/S2053273317016540>.
- [3] S.J. Ahn, P. Moon, T.-H. Kim, H.-W. Kim, H.-C. Shin, E.H. Kim, H.W. Cha, S.-J. Kahng, P. Kim, M. Koshino, Y.-W. Son, C.-W. Yang, J.R. Ahn, Dirac electrons in a dodecagonal graphene quasicrystal, Science. 361 (6404) (2018) 782–786, <https://doi.org/10.1126/science:aar8412>.
- [4] W. Yao, E. Wang, Y. Zhang, K. Zhang, C.K. Chan, C. Chen, J. Avila, M.C. Asensio, J. Zhu, S. Zhou, Quasicrystalline 30° twisted bilayer graphene as an incommensurate superlattice with strong interlayer coupling, Proc Natl Acad Sci USA 115 (2018) 6, <https://doi.org/10.1073/pnas.1720865115>.
- [5] S. Pezzini, V. Mišekis, G. Piccinini, S. Forti, S. Pace, R. Engelke, F. Rossella, K. Watanabe, T. Taniguchi, P. Kim, C. Coletti, 30° -Twisted Bilayer Graphene Quasicrystals from Chemical Vapor Deposition, Nano Lett. 20 (5) (2020) 3313–3319, <https://doi.org/10.1021/acs.nanolett.0c00172>.
- [6] E. Koren, U. Duerig, Superlubricity in quasicrystalline twisted bilayer graphene, Phys. Rev. B. 93 (2016), 201404, <https://doi.org/10.1103/PhysRevB.93.201404>.
- [7] K.S. Novoselov, Electric Field Effect in Atomically Thin Carbon Films, Science. 306 (5696) (2004) 666–669, <https://doi.org/10.1126/science.1102896>.
- [8] J.D. Cain, A. Azizi, M. Conrad, S.M. Griffin, A. Zettl, Layer-dependent topological phase in a two-dimensional quasicrystal and approximant, Proc Natl Acad Sci USA 117 (42) (2020) 26135–26140, <https://doi.org/10.1073/pnas.2015164117>.
- [9] T.P. Yadav, C.F. Woellner, T. Sharifi, S.K. Sinha, L.-I. Qu, A. Apte, N. K. Mukhopadhyay, O.N. Srivastava, R. Vajtai, D.S. Galvão, C.S. Tiwary, P. M. Ajayan, Extraction of Two-Dimensional Aluminum Alloys from Decagonal Quasicrystals, ACS Nano. 14 (6) (2020) 7435–7443, <https://doi.org/10.1021/acsnano.0c03081>.
- [10] P. Stampfli, A Dodecagonal Quasiperiodic Lattice in Two Dimensions, Helv. Phys. Acta. 56 (1986) 1260–1263.
- [11] P. Moon, M. Koshino, Y.-W. Son, Quasicrystalline electronic states in 30° rotated twisted bilayer graphene, Phys. Rev. B. 99 (2019), 165430, <https://doi.org/10.1103/PhysRevB.99.165430>.
- [12] G. Yu, Z. Wu, Z. Zhan, M.I. Katsnelson, S. Yuan, Dodecagonal bilayer graphene quasicrystal and its approximants, Npj Comput Mater. 5 (2019) 122, <https://doi.org/10.1038/s41524-019-0258-0>.
- [13] G. Yu, M.I. Katsnelson, S. Yuan, Pressure and electric field dependence of quasicrystalline electronic states in 30° twisted bilayer graphene, Phys. Rev. B. 102 (2020), 045113, <https://doi.org/10.1103/PhysRevB.102.045113>.
- [14] F. Piazza, K. Gough, M. Monthoux, P. Puech, I. Gerber, R. Wiens, G. Paredes, C. Ozoria, Low temperature, pressureless sp^2 to sp^3 transformation of ultrathin, crystalline carbon films, Carbon. 145 (2019) 10–22, <https://doi.org/10.1016/j.carbon.2019.01.017>.
- [15] P.V. Bakharev, M. Huang, M. Saxena, S.W. Lee, S.H. Joo, S.O. Park, J. Dong, D. C. Camacho-Mojica, S. Jin, Y. Kwon, M. Biswal, F. Ding, S.K. Kwak, Z. Lee, R. S. Ruoff, Chemically induced transformation of chemical vapour deposition grown bilayer graphene into fluorinated single-layer diamond, Nature Nanotechnology. 15 (1) (2020) 59–66, <https://doi.org/10.1038/s41565-019-0582-z>.
- [16] F. Piazza, Kelvin Cruz, M. Monthoux, P. Puech, I. Gerber, Raman evidence for the successful synthesis of diamane, Carbon. 169 (2020) 129–133, <https://doi.org/10.1016/j.carbon.2020.07.068>.
- [17] L.A. Chernozatonskii, P.B. Sorokin, A.G. Kvashnin, Diamond-like C₂H nanolayer, diamane: Simulation of the structure and properties, JETP Letters. 90 (2) (2009) 134–138, <https://doi.org/10.1134/S0021364009140112>.
- [18] A.G. Kvashnin, P.B. Sorokin, Lonsdaleite Films with Nanometer Thickness, J. Phys. Chem. Lett. 5 (3) (2014) 541–548, <https://doi.org/10.1021/jz402528q>.
- [19] L.A. Chernozatonskii, P.B. Sorokin, A.A. Kuzubov, B.P. Sorokin, A.G. Kvashnin, D. G. Kvashnin, P.V. Avramov, B.I. Yakobson, Influence of Size Effect on the Electronic and Elastic Properties of Diamond Films with Nanometer Thickness, The Journal of Physical Chemistry C. 115 (1) (2011) 132–136, <https://doi.org/10.1021/jp1080687>.
- [20] A.G. Kvashnin, L.A. Chernozatonskii, B.I. Yakobson, P.B. Sorokin, Phase Diagram of Quasi-Two-Dimensional Carbon, From Graphene to Diamond, Nano Letters. 14 (2) (2014) 676–681, <https://doi.org/10.1021/n403938g>.
- [21] Y. Gao, T. Cao, F. Cellini, C. Berger, W.A. de Heer, E. Tosatti, E. Riedo, A. Bongiorno, Ultrahard carbon film from epitaxial two-layer graphene, Nature Nanotech. 13 (2) (2018) 133–138, <https://doi.org/10.1038/s41565-017-0023-9>.
- [22] L.A. Chernozatonskii, V.A. Demin, D.G. Kvashnin, Ultrawide-bandgap Moiré diamanes based on bigraphenes with the twist angles $\Theta \sim 30^\circ$, Appl. Phys. Lett. 117 (25) (2020) 253104, <https://doi.org/10.1063/5.0027839>.
- [23] A.R. Muniz, D. Maroudas, Opening and tuning of band gap by the formation of diamond superlattices in twisted bilayer graphene, Phys. Rev. B. 86 (2012), 075404, <https://doi.org/10.1103/PhysRevB.86.075404>.
- [24] M. Chen, A.R. Muniz, D. Maroudas, Formation and Mechanical Behavior of Nanocomposite Superstructures from Interlayer Bonding in Twisted Bilayer Graphene, ACS Applied Materials & Interfaces. 10 (34) (2018) 28898–28908, <https://doi.org/10.1021/acsami.8b09741>.
- [25] W.L. Mao, Bonding Changes in Compressed Superhard Graphite, Science. 302 (5644) (2003) 425–427, <https://doi.org/10.1126/science.1089713>.
- [26] S. Rajasekaran, F. Abild-Pedersen, H. Ogasawara, A. Nilsson, S. Kaya, Interlayer Carbon Bond Formation Induced by Hydrogen Adsorption in Few-Layer Supported Graphene, Phys. Rev. Lett. 111 (2013), 085503, <https://doi.org/10.1103/PhysRevLett.111.085503>.
- [27] A.P.M. Barboza, M.H.D. Guimaraes, D.V.P. Massote, L.C. Campos, N.M. Barbosa Neto, L.G. Cancado, R.G. Lacerda, H. Chacham, M.S.C. Mazzoni, B.R.A. Neves, Room-Temperature Compression-Induced Diamondization of Few-Layer Graphene,

- Advanced Materials. 23 (27) (2011) 3014–3017, <https://doi.org/10.1002/adma.201101061>.
- [28] D.K. Samarakoon, X.-Q. Wang, Tunable Band Gap in Hydrogenated Bilayer Graphene, ACS Nano. 4 (7) (2010) 4126–4130, <https://doi.org/10.1021/nm1007868>.
- [29] D. Odkhuu, D. Shin, R.S. Ruoff, N. Park, Conversion of multilayer graphene into continuous ultrathin sp₃-bonded carbon films on metal surfaces, Sci Rep. 3 (2013) 3276, <https://doi.org/10.1038/srep03276>.
- [30] H. Touhara, K. Kadono, Y. Fujii, N. Watanabe, On the Structure of Graphite Fluoride, Zeitschrift Für Anorganische Und Allgemeine Chemie. 544 (1) (1987) 7–20, <https://doi.org/10.1002/zaac.19875440102>.
- [31] J. Sivek, O. Leenaerts, B. Partoens, F.M. Peeters, First-Principles Investigation of Bilayer Fluorographene, The Journal of Physical Chemistry C. 116 (36) (2012) 19240–19245, <https://doi.org/10.1021/jp3027012>.
- [32] A.G. Kvashnin, P.V. Avramov, D.G. Kvashnin, L.A. Chernozatonskii, P.B. Sorokin, Features of Electronic, Mechanical, and Electromechanical Properties of Fluorinated Diamond Films of Nanometer Thickness, J. Phys. Chem. C. 121 (51) (2017) 28484–28489, <https://doi.org/10.1021/acs.jpcc.7b07946>.
- [33] S.M. Clark, K.-J. Jeon, J.-Y. Chen, C.-S. Yoo, Few-layer graphene under high pressure: Raman and X-ray diffraction studies, Solid State Communications. 154 (2013) 15–18, <https://doi.org/10.1016/j.ssc.2012.10.002>.
- [34] F. Ke, L. Zhang, Y. Chen, K. Yin, C. Wang, Y.-K. Tzeng, Y.u. Lin, H. Dong, Z. Liu, J. S. Tse, W.L. Mao, J. Wu, B. Chen, Synthesis of Atomically Thin Hexagonal Diamond with Compression, Nano Letters. 20 (8) (2020) 5916–5921, <https://doi.org/10.1021/acs.nanolett.0c01872>.
- [35] L.A. Chernozatonskii, V.A. Demin, D.G. Kvashnin, Fully Hydrogenated and Fluorinated Bigraphenes-Diamanes: Theoretical and Experimental Studies, C. 7 (2021) 17, <https://doi.org/10.3390/c7010017>.
- [36] G. Kresse, J. Furthmüller, Efficiency of ab-initio total energy calculations for metals and semiconductors using a plane-wave basis set, Computational Materials Science. 6 (1) (1996) 15–50, [https://doi.org/10.1016/0927-0256\(96\)00008-0](https://doi.org/10.1016/0927-0256(96)00008-0).
- [37] G. Kresse, J. Hafner, Ab initio molecular dynamics for liquid metals, Phys. Rev. B. 47 (1) (1993) 558–561, <https://doi.org/10.1103/PhysRevB.47.558>.
- [38] G. Kresse, J. Hafner, Ab initio molecular-dynamics simulation of the liquid-metal–amorphous-semiconductor transition in germanium, Phys. Rev. B. 49 (20) (1994) 14251–14269, <https://doi.org/10.1103/PhysRevB.49.14251>.
- [39] J.P. Perdew, K. Burke, M. Ernzerhof, Generalized Gradient Approximation Made Simple, Phys. Rev. Lett. 77 (18) (1996) 3865–3868, <https://doi.org/10.1103/PhysRevLett.77.3865>.
- [40] P.E. Blöchl, Projector augmented-wave method, Phys. Rev. B. 50 (24) (1994) 17953–17979, <https://doi.org/10.1103/PhysRevB.50.17953>.
- [41] G. Kresse, D. Joubert, From ultrasoft pseudopotentials to the projector augmented-wave method, Phys. Rev. B. 59 (3) (1999) 1758–1775, <https://doi.org/10.1103/PhysRevB.59.1758>.
- [42] C.D. Clark, P.J. Dean, P.V. Harris, W.C. Price, Intrinsic edge absorption in diamond, Proceedings of the Royal Society of London. Series A. Mathematical and Physical Sciences. 277 (1964) 312–329, <https://doi.org/10.1098/rspa.1964.0025>.
- [43] S.J. Stuart, A.B. Tutein, J.A. Harrison, A reactive potential for hydrocarbons with intermolecular interactions, The Journal of Chemical Physics. 112 (14) (2000) 6472–6486, <https://doi.org/10.1063/1.481208>.
- [44] S. Plimpton, Fast Parallel Algorithms for Short-Range Molecular Dynamics, Journal of Computational Physics. 117 (1) (1995) 1–19, <https://doi.org/10.1006/jcph.1995.1039>.
- [45] L.i. Song, L. Ci, H. Lu, P.B. Sorokin, C. Jin, J. Ni, A.G. Kvashnin, D.G. Kvashnin, J. Lou, B.I. Yakobson, P.M. Ajayan, Large Scale Growth and Characterization of Atomic Hexagonal Boron Nitride Layers, Nano Lett. 10 (8) (2010) 3209–3215, <https://doi.org/10.1021/nl1022139>.
- [46] L. Hornekær, Ž. Šljivančanin, W. Xu, R. Otero, E. Rauls, I. Stensgaard, E. Lægsgaard, B. Hammer, F. Besenbacher, Metastable Structures and Recombination Pathways for Atomic Hydrogen on the Graphite (0001) Surface, Phys. Rev. Lett. 96 (2006), 156104, <https://doi.org/10.1103/PhysRevLett.96.156104>.
- [47] H. Li, T. Duan, S. Haldar, B. Sanyal, O. Eriksson, H. Jafri, S. Hajjar-Garreau, L. Simon, K. Leifer, Direct writing of lateral fluorographene nanopatterns with tunable bandgaps and its application in new generation of moiré superlattice, Applied Physics Reviews. 7 (1) (2020) 011403, <https://doi.org/10.1063/1.5129948>.
- [48] L.A. Chernozatonskii, K.P. Katin, V.A. Demin, M.M. Maslov, Moiré diamanes based on the hydrogenated or fluorinated twisted bigraphene: The features of atomic and electronic structures, Raman and infrared spectra, Applied Surface Science. 537 (2021) 148011, <https://doi.org/10.1016/j.apsusc.2020.148011>.
- [49] Z. Zeng, L. Yang, Q. Zeng, H. Lou, H. Sheng, J. Wen, D.J. Miller, Y. Meng, W. Yang, W.L. Mao, H. Mao, Synthesis of quenchable amorphous diamond, Nat Commun. 8 (2017), 322, <https://doi.org/10.1038/s41467-017-00395-w>.
- [50] C. Lee, X. Wei, J.W. Kysar, J. Hone, Measurement of the Elastic Properties and Intrinsic Strength of Monolayer Graphene, Science. 321 (5887) (2008) 385–388, <https://doi.org/10.1126/science.1157996>.
- [51] G. Lopez-Polin, C. Gomez-Navarro, V. Parente, F. Guinea, M.I. Katsnelson, F. Perez-Murano, J. Gomez-Herrero, Increasing the elastic modulus of graphene by controlled defect creation, Nature Physics. 11 (2015) 26–31, <https://doi.org/10.1038/nphys3183>.
- [52] H. Shu, Strain effects on stability, electronic and optical properties of two-dimensional C₄X₂ (X = F, Cl, Br), J. Mater. Chem. C. 9 (13) (2021) 4505–4513, <https://doi.org/10.1039/DITC00507C>.